TDF-TRACT: PROBABILISTIC TRACTOGRAPHY USING THE TENSOR DISTRIBUTION FUNCTION

J.J. GadElkarim[1,2], L. Zhan[3], S.L. Yang[1], A.F. Zhang[1], L. Altshuler[4], M. Lamar[1], O. Ajilore[1]
P.M. Thompson[3], A. Kumar[1], A. Leow[1,5]

[1]Department of Psychiatry, University of Illinois-Chicago
[2]Department of Electrical and Computer Engineering, University of Illinois-Chicago
[3]Laboratory of Neuro Imaging, UCLA School of Medicine
[4]Neuropsychiatric Institute, UCLA School of Medicine, Los Angeles, CA
[5]Community Psychiatry Associates, Sacramento, CA

ABSTRACT

Fractional anisotropy (FA), a widely used measure of fiber integrity based on diffusion tensor imaging (DTI), is theoretically confounded by several other quantities including the degree of fiber orientation incoherence within each voxel, and partial volume effects from neighboring gray matter or CSF. High angular resolution diffusion imaging (HARDI) can potentially resolve more complex diffusion geometries and thus disentangle confounds from fiber incoherence and partial voluming when assessing fiber integrity. Yet, to date, no study has systematically investigated the clinical implications of this potential advantage. Here, we describe our recent efforts in developing TDF (tensor distribution function) based probabilistic tractography for HARDI. Comparing TDF- and DTI-based tractography results in the *genu* of corpus callosum, we demonstrated the variable effect of these confounds in images acquired at different spatial resolutions, suggesting possible relevance of adjusting for fiber incoherence when assessing white matter integrity.

Index Terms— High-Angular Resolution Diffusion Imaging; Diffusion tensor imaging; Fractional Anisotropy.

1. INTRODUCTION

Diffusion-weighted MRI is a powerful tool to study water diffusion in tissue, providing vital information on white matter microstructure, such as fiber connectivity and integrity in the healthy and diseased brain. The *diffusion tensor imaging* (DTI) model [1, 2] describes the anisotropy of water diffusion in tissues. It estimates, from a set of K diffusion-sensitized images, the 3x3 *diffusion tensor* (the covariance matrix of a 3-dimensional Gaussian distribution). In this single-tensor diffusion model, each voxel's signal intensity in the k-th image is attenuated, by water diffusion, according to the Stejskal-Tanner equation [3]: $S_k = S_0 \, exp\,[-b\mathbf{g_k}^T \mathbf{D}\, \mathbf{g_k}]$, where S_0 is the non-diffusion weighted signal intensity, $\mathbf{D}$ is the 3x3 diffusion tensor, $\mathbf{g_k}$ is the diffusion gradient direction and b is Le Bihan's factor containing information on the pulse sequence, gradient strength, and physical constants. Seven independent gradients are mathematically sufficient to determine the diffusion tensor, but MRI protocols with higher angular and radial resolutions, such as high-angular resolution diffusion imaging (HARDI) or diffusion spectrum imaging [4-12], have been proposed to resolve more complex diffusion geometries, such as fiber crossings and intermixing of tracts.

Much progress has been made in modeling various degrees of fiber incoherence with HARDI, but most clinical studies still rely on simple DTI-derived measures such as the fractional anisotropy (FA; a commonly used measure of white matter integrity) and mean diffusivity (MD). One plausible explanation for such reluctance to embrace HARDI is that there has been no systematic effort investigating how the theoretical confound of fiber incoherence impacts clinical research. In this study, we seek to provide evidence showing that fiber incoherence confound is highly relevant and anything but negligible. In particular, we will show the following:

1. FA values of the same brain structure heavily depend on the spatial resolution during image acquisition, making their interpretation questionable and comparisons across studies problematic.
2. This dependence is mostly due to the higher degree of fiber incoherence in lower spatial resolution scans due to partial voluming. A measure with such high dependence on scanning parameters is questionable in quantifying underlying physiology.
3. Such dependence can be mostly overcome by HARDI-based analysis methods.

2. METHODS

2.1. Data acquisition

Two sets of 32-direction diffusion-weighted images (DWI) were acquired from an individual subject using single-shot spin-echo echo-planar imaging (EPI) sequence from Philips Achieva 3.0 T scanner with an 8-channel head-coil at the UIMC (University of Illinois Medical Center) Advanced Imaging Center. The two 32-direction volumes were acquired back-to-back in one single session with minimal subject movement. The two scans used identical parameters except for the final reconstructed volume sizes (the low resolution at 2.14mm x 2.14mm versus the higher "reconstructed" resolution at 0.83mm X 0.83 in-plane). The following parameters were used: b = 700s/mm^2, FOV=240 mm, in-plane resolution: 2.14mm x 2.14mm, slice thickness 2.2 mm, no gap, 68 axial slices, TR=6994ms and TE=71ms and Flip angle 90^o (total scan time: 4 min11s per scan; parallel imaging was also utilized with a SENSE factor of 2 to reduce scanning time). The 32 gradient directions are consistent with the default setting in DTI Studio (http://cmrm.med.jhmi.edu/; a widely distributed program developed by researchers at the Johns Hopkins University led by Prof. Susumu Mori), and are commonly used by the neuroimaging community.

2.2. Data processing

To reconstruct standard DTI, a positive definite diffusion tensor was estimated at each voxel from the raw data using the DTI Studio software, followed by deterministic tractography. Based on the diffusion tensor eigenvalues (λ_1, λ_2, and λ_3), the standard FA (denoted as FA^{DTI} to avoid confusion) is defined as:

$$FA^{DTI} = \sqrt{\frac{1}{2}\left(\frac{(\lambda_1-\lambda_2)^2+(\lambda_2-\lambda_3)^2+(\lambda_3-\lambda_1)^2}{\lambda_1^2+\lambda_2^2+\lambda_3^2}\right)} \quad (1)$$

Its values range from 0 (no directional dependence of diffusion) to 1 (diffusion along a single direction). Concurrently, in addition to standard DTI, we applied the TDF framework [13] to the same data, computing a probabilistic ensemble of 3D Gaussian diffusion processes at each voxel that best describes the observed signal. Briefly, in the TDF approach, a Tensor Distribution Function P defined on the tensor space $\overline{D}$ is computed to explain the diffusion-weighted images using the least squared-error principle (with respect to the observed signals S_{obs}):

$$\begin{aligned} S_{calculated}(q) &= \int_{D\in\overline{D}} P(D)\exp(-tq^t Dq)dD \\ P^* &= \arg\min_p \sum_i (S_{obs}(q_i) - S_{calculated}(q_i))^2 \end{aligned} \quad (2)$$

As the solution space is a six-parameter space (3 eigenvalues plus 3 angles), some dimension reduction is helpful for numerical optimization. We assume that fiber tracts are cylindrical by enforcing two eigenvalues of each individual tensor to be equal. Thus, $\lambda_1 \geq \lambda_2 = \lambda_3$ for each individual tensor. Given any tensor distribution function, *P,* the dominant fiber orientations may be estimated by examining the local maxima of the tensor orientation distribution (TOD). The TOD is defined as the marginal density of TDF with respect to the spherical angle:

$$TOD(\theta) = \int_{\lambda} P(D(\lambda,\theta))d\lambda \quad (3)$$

With Eq. (3), TDF-based probabilistic tractography can now be performed by following trajectories originating from selected ROIs by randomly sampling the local TOD profiles. The procedure is similar to ODF (orientation distribution function) based HARDI tractography (e.g., [14]). However, instead of sampling the ODF to determine fiber tract directions, we sample the TOD profile. This has several advantages. First, unlike the ODF, the TOD has sharp and distinct local maxima at the estimated dominant fiber directions (with the ODF, however, the water diffusion profile is collapsed onto the unit sphere using radial integration). As a result, the ODF has a relatively flat profile and is unsuitable for tractography without some pre-processing (e.g., the 'min-max" operation [4]). The pre-processing is thus designed to "sharpen" the ODF profile. By contrast, directly sampling the TOD renders the tractography much more precise and may reduce the likelihood of recovering erroneous fiber tracts. In our implementation, the step size is set to be 0.25, and a maximum bending angle is set between 50-60 degrees. The fiber tracts are built in both directions until reaching voxels where dominant diffusion direction can no longer be determined (i.e., gray matter as operationally defined using the TDF). The resulting algorithm, called TDF-TRACT, is probabilistic in nature, so tracts are constructed with multiple repeats at each seed point. We found that 10-100 repeats with random initiations inside the seed voxel are usually sufficient to extract all major white matter tracts.

The TDF-corrected eigenvalues ($\overline{\lambda_1}, \overline{\lambda_2}$) are determined by computing the expected values of the eigenvalues with respect to the tensor distribution function P, and thus mathematically average the eigenvalues of all estimated dominant fiber directions:

$$\overline{\lambda_i} = \int P(D(\lambda,\theta))\lambda_i d\lambda d\theta \quad (4)$$

The TDF-corrected FA is defined as the FA value computed using the TDF-corrected eigenvalues and thus provide an overall assessment of anisotropy by decomposing the fiber incoherence confound.

Lastly, we propose the circular standard deviation (CSD), a quantity that can be found in classical theories on directional statistics (see, for example [5]), as a measure of fiber incoherence. At each voxel, given the TOD, CSD is computed via the mean fiber direction (R) of all detected fiber directions (the Z^is) as follows:

$$\begin{cases} \mathrm{R} = \sum_{\mathrm{i}} TOD(Z^i).Z^i d\theta \\ CSD = \sqrt{-2\log(\|R\|)} \end{cases} \quad (5)$$

Where the ||.|| sign denotes the Euclidian norm.

3. RESULTS AND DISCUSSION

3.1 Graphical user interface for TDF-tractography

The graphical user interface (GUI) for our TDF-TRACT program, is shown in **Figure 1**. It is implemented in the Matlab environment. The user interface has the capabilities of displaying the TOD along with the colored fiber orientation (e.g., red denotes left-right orientation), as well as various slice views of the corresponding structural image. This allows the user to easily navigate between structural anatomy and local fiber directional information, making it easier to identify and trace ROIs. Similar to DTI Studio, the "and/not" function is implemented such that the user may perform virtual dissections of white matter structures, in an interactive manner. In addition, the user may specify the number of random samplings of trajectories per seed point. **Figure 1** shows the procedure we used to extract commissural fibers in the *corpus callosum*, by first identifying the mid-sagittal TOD (*upper left panel*) relative to the anatomy (*upper middle panel*) followed by placing a seed region tracing the contour of corpus callosum in the TOD space. The tracts were then visualized in the "tract view" overlaid on the structural image (*lower left panel*).

3.2 Standard versus TDF-corrected FA

To demonstrate that the standard FA values are heavily confounded by the degree of fiber orientational incoherence, we constructed the corpus callosum fibers in the *genu* region for data at both spatial resolutions using DTI Studio using the procedure described in Figure 1. The commissural fibers in the *genu* have been previously studied: in [15, 16], the FA values along the fiber

tracts were computed and plotted against their geodesic distance from the midline point. There, the authors investigated early neonatal development of the corpus callosum using DTI measures including FA, by plotting and assessing regional longitudinal changes of FA values. Interestingly, in the results the authors commented that "**FA seems to be more dependent on tract organization, whereas MD seems to be more sensitive to myelination**", which is consistent with our hypotheses.

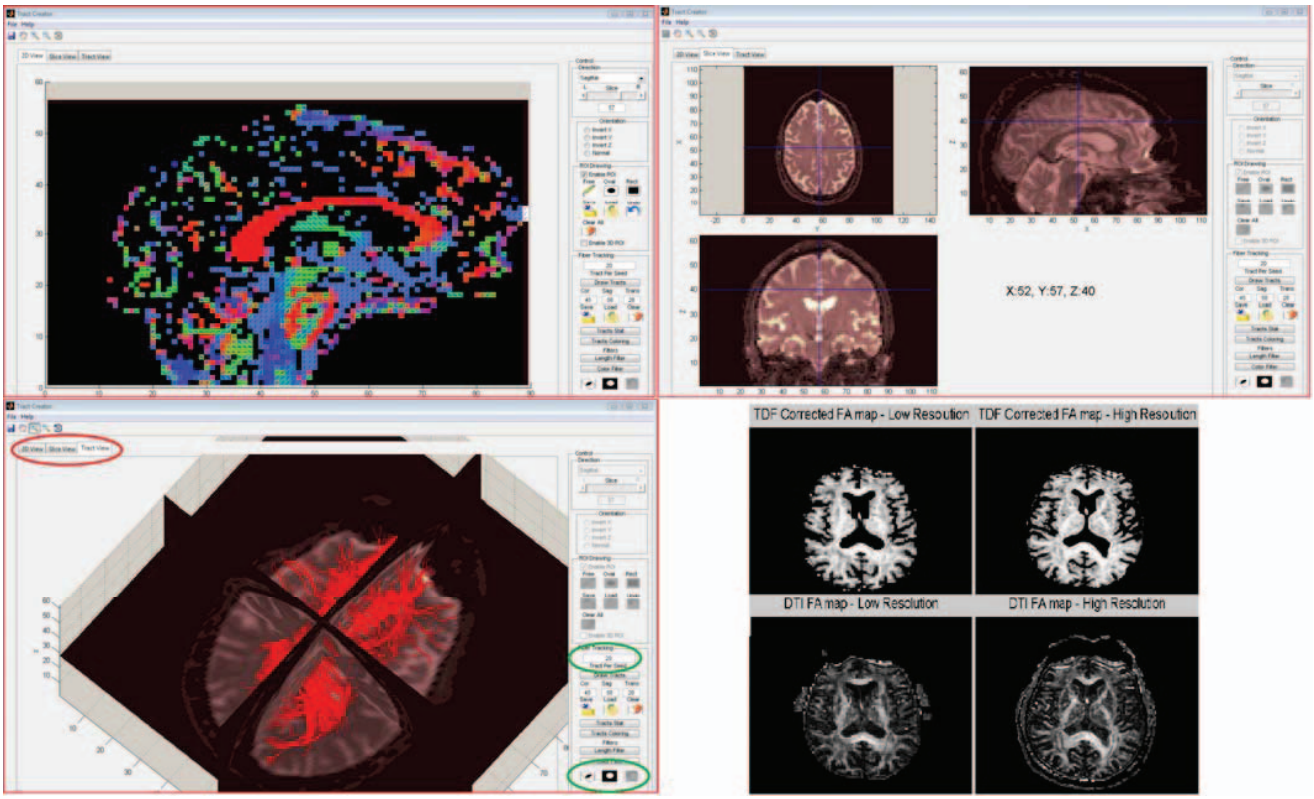

Figure 1. Here the GUI for the TDF-TRACT program is shown. There are three available views: the TOD view (*upper left panel*), slice view (*upper right panel*), and the tract view (*lower left*). TDF-TRACT also implements the "and/not" function, and users may specify the number of probabilistic tracts per seed (*highlighted in red and green circles*). As in DTI Studio, the user may perform virtual dissections of white matter structures in an interactive fashion, by switching among these three views. Here the three views show how commissural fibers originating from the *genu* are extracted and displayed. The lower right panel shows an axial slice of the four different FA maps studied in this paper.

Following the same analyses, in Figure 2 we plot the average FA values (from DTI Studio) against this geodesic distance, across all reconstructed commissural fibers, for both the high and low spatial resolution data. Although the raw data were acquired in one single session on the same subject using the same parameters except for the final reconstructed volume, FA values are substantially higher for the higher spatial resolution data, especially in the central portion of the plot. We hypothesize that such an increase of FA values is due to the lower fiber incoherence, within each voxel, as a result of the higher spatial resolution. Indeed, around the genu, commissural fibers curve and roughly trace the trajectory of a semi-circle, and thus a larger voxel would capture more this curving trajectory, leading to a higher degree of incoherence. Also, here we note in passing that FA, being a measure of such strong dependence on image spatial resolution is thus problematic in quantifying underlying physiology.

To further investigate this surprisingly large difference in FA values, **Figure 3** plots the TDF-corrected FA versus the standard DTI FA for both datasets. The commissural tracts used to compute TDF-corrected FA were generated using the in-house TDF-tractography program. Here, we notice that for the low resolution dataset, TDF-corrected FA also has values much higher than the non-corrected FA, supporting that the low FA values in low spatial resolution data is a direct result of the higher degree of fiber incoherence due to the larger voxel size. In addition, TDF-corrected FA values appear to have minimal dependence on the spatial resolution, thus confirming their theoretical advantage over their standard DTI counterparts.

Indeed, if this FA variability in standard DTI is mostly a result of fiber incoherence, we might expect, at least for the low spatial resolution data, that CSD would closely follow the opposite effects to FA with respect to the geodesic distance (i.e., high degree of fiber incoherence leads to higher CSD values but lower FA values). Not surprisingly, plotting CSD and DTI-FA against

geodesic distance for the lower resolution data confirms this (**Figure 4**). The dotted blue line of the FA closely follows the trend of the inverse CSD (*red line*).

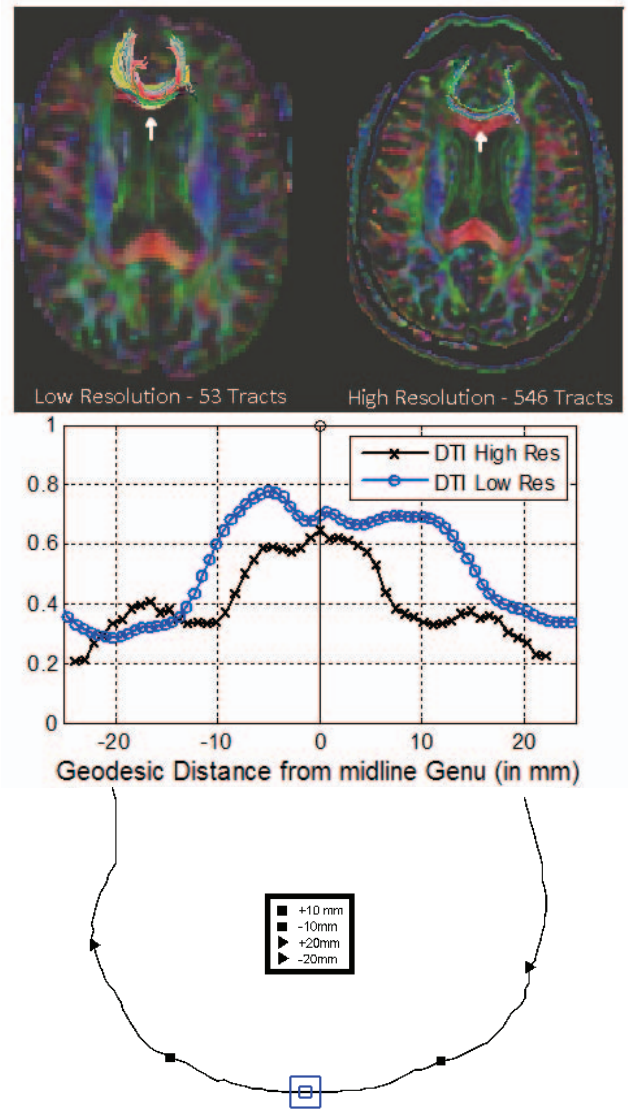

Figure 2 plots the averaged FA values (*second panel*) with respect to the geodesic distance from the mid-sagittal point (marked with white arrows, *top panel*) across all reconstructed commissural fibers in the genu of corpus callosum (*top panel*). Although the two sets of raw data were acquired in one single session on the same subject using the same parameters except for the final reconstructed volume, we notice that the FA values are much higher for the higher spatial resolution data, especially in the central portion of the plot (i.e., around the mid-sagittal point). All results in this figure were produced using the DTI Studio software. *Third panel* shows the mid-sagittal point, the geodesic distance, and the low and high spatial resolution voxel sizes (the blue squares) with respect to a typical commissural fiber in the genu of corpus callosum.

4. CONCLUSION

Using two sets of DTI/HARDI data acquired from one human subject scanned in a single MRI session using the same parameters except for the final reconstructed spatial resolution, we showed that FA values depend heavily on the spatial resolution of the final reconstructed images. In particular, the average FA values of commissural fibers around the genu varied from 0.3-0.4 using the low-resolution data, to 0.6-0.8 using the high resolution data. As one expects the neuroanatomy and its physiology to stay the same, for all intents and purposes, during a one-hour scan session, one can conclude that standard FA derived from DTI may not be clinically acceptable in quantifying the underlying physiological properties of white matter such as myelination, as is widely and generally assumed.

Future imaging studies of white matter integrity may benefit from adopting HARDI-based analyses to better disentangle various confounds contributing to standard FA as a measure of fiber integrity.

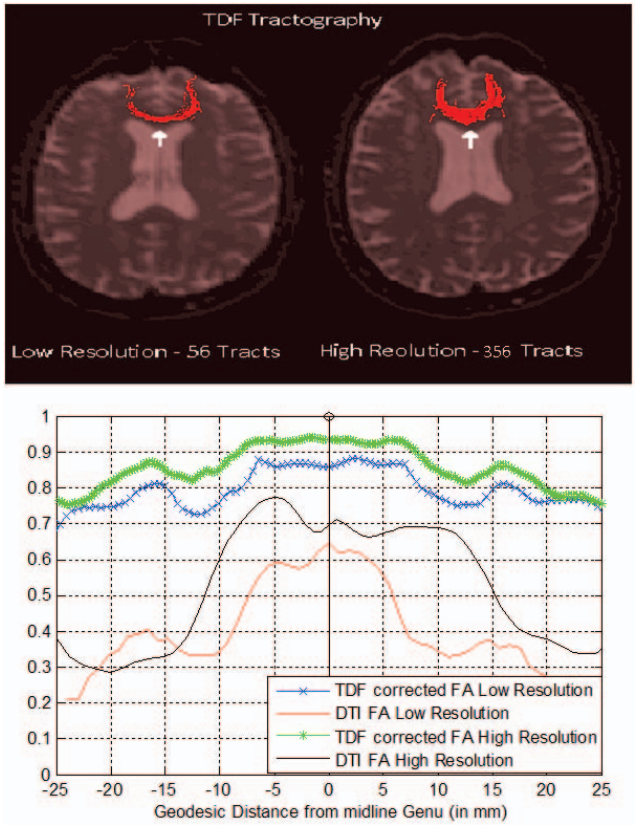

Figure 3 plots the TDF-corrected FA versus the standard DTI FA for both low and high resolution data (*lower panel*). Tracts were generated using our TDF-tractography program, and used to extract TDF-corrected FA values along the curves (*upper panel*). Here, we notice that for the low resolution dataset, TDF-corrected FA also has values higher than the non-corrected FA. Moreover, TDF-corrected FA has minimal dependence on the spatial resolution. This supports our hypothesis that the low FA values in low spatial resolution data are a direct result of the higher degree of fiber incoherence due to the larger voxel size.

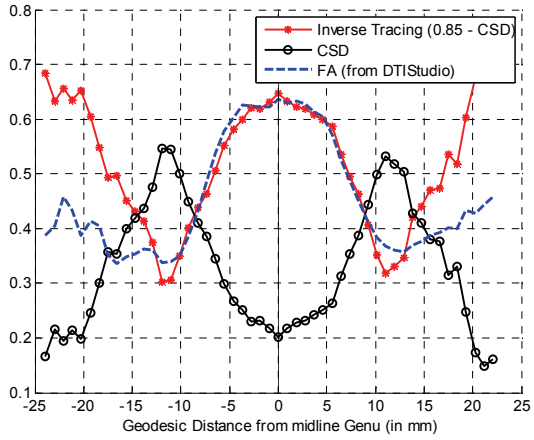

Figure 4 plots the CSD and average DTI-derived FA against the geodesic distance from the mid-sagittal point, across all reconstructed fibers, for the low spatial resolution data. The CSD is interpreted as a measure of the degree of fiber incoherence. Here, the FA tracing (*dotted blue line*) closely follows the trend of the inverse CSD tracing (*red line*) within 15mm from the mid-sagittal point. Thus, FA values along tracts are highly correlated with, and dependent upon, the degree of fiber incoherence. This is more pronounced in lower spatial resolution images.

5. REFERENCES

1. Basser PJ, Pierpaoli C. Microstructural and physiological features of tissues elucidated by quantitative diffusion tensor MRI. J. Magn. Reson. vol. B 111, no. 3, pp.209-219, 1996.
2. Le Bihan D. Magnetic resonance imaging of perfusion. Magn Reson Med. 14(2):283-92, 1990.
3. Stejskal EO, Tanner JE. Spin diffusion measurements: spin echoes in the presence of a time-dependent field gradient. J. Chem. Phys. 42:288-292, 1965.
4. Tuch DS, Q-Ball Imaging. Magnetic Resonance in Medicine 52:1358-1372, 2004.
5. Directional Statistics, http://en.wikipedia.org/wiki/Directional_statistics
6. Hess CP, Mukherjee P, Han ET, Xu D, Vigneron DB. Q-ball reconstruction of multimodal fiber orientations using the spherical harmonic basis. Magn Reson Med. 56: 104-117, 2006.
7. Jansons KM, Alexander DC. Persistent angular structure: new insights from diffusion magnetic resonance imaging data. Inverse Probl; 19: 1031-1046, 2003.
8. Anderson AW. Measurement of fiber orientation distributions using high angular resolution diffusion imaging. Magn Reson Med.; 54: 1194-1206, 2005.
9. Özarslan E, Shepherd T, Vemuri BC, Blackband S, Mareci T. Resolution of complex tissue microarchitecture using the diffusion orientation transform (DOT). NeuroImage; 31(3): 1083–1106, 2006.
10. Tournier JD, Calamante F, Gadian D, Connelly A. Direct estimation of the fiber orientation density function from diffusion-weighted MRI data using spherical deconvolution. NeuroImage, 23:1176–1185, 2004.
11. Alexander DC. Maximum entropy spherical deconvolution for diffusion MRI. In: Proceedings of the 19th International Conference on Information Processing in Medical Imaging (IPMI), Glenwood Springs, CO, USA; 2005.
12. Kaden E, Knösche TR, Anwander A. Parametric spherical deconvolution: Inferring anatomical connectivity using diffusion MR imaging. Neuroimage. 37: 474-488, 2007.
13. Leow AD, Zhu S, Zhan L, de Zubicaray GI, Meredith M, Wright M, Toga AW, Thompson PM. The Tensor Distribution Function, Magn Reson Med. 18; 61(1):205-214, 2008.
14. Descoteaux, M., Deriche, R., Knosche, T.R., Anwander, A. Deterministic and Probabilistic Tractography Based on Complex Fibre Orientation Distributions. IEEE-TMI 28(2): 269-286, 2009
15. Pierre Fillard, John Gilmore, Joseph Piven, Weili Lin, Guido Gerig Quantitative Analysis of White Matter Fiber Properties along Geodesic Paths. *Proc. MICCAI*, LNCS 2879: 16-23, 2003.
16. J.H. Gilmore, W. Lin, I. Corouge, Y.S.K. Vetsa, J.K. Smith, C. Kanga, H. Gua, R.M. Hamera, J.A. Lieberman and G. Gerig Early Postnatal Development of Corpus Callosum and Corticospinal White Matter Assessed with Quantitative Tractography. *American Journal of Neuroradiology* 28:1789-1795, October 2007.
17. Pierpaoli, C., Jezzard, P., Basser, P.J., Barnett, A., and Chiro, G. Diffusion tensor MR imaging of the human brain. Radiology 201:637-648, 1996.